Structural Characterization of Mononuclear Cu(II) and Its Nitrite Complex in the Active Site of *Carcinus maenas* Hemocyanin†

Luigi Bubacco,*,‡ Richard S. Magliozzo,§ Michael D. Wirt,§ Mariano Beltramini,|| Benedetto Salvato,|| and Jack Peisach‡,§

Department of Physiology and Biophysics and Department of Molecular Pharmacology, Albert Einstein College of Medicine of Yeshiva University, Bronx, New York 10461, and Department of Biology and Center for the Biochemistry and Physiology of Hemocyanins and Other Metalloproteins, University of Padua, 35131, Padua, Italy

Received June 27, 1994; Revised Manuscript Received November 8, 1994⊗

ABSTRACT: The preparation of a mononuclear Cu(II) derivative of *Carcinus maenas* hemocyanin (Cu(II)-Hc) and a nitrite complex of the derivative (Cu(II)-Hc-NO_2^-) are described. Several techniques have been used in their characterization, including X-ray absorption, continuous wave (cw) EPR, and electron spin−echo envelope modulation (ESEEM) spectroscopies. EXAFS results for Cu(II)-Hc indicate the presence of three ligands at 1.99 ± 0.01 Å and a fourth one at 2.26 ± 0.01 Å from the copper. The same coordination number and very similar bond lengths were obtained for Cu(II)-Hc-NO_2^-. On the basis of simulations of three-pulse ESEEM spectra, three equivalent imidazole nitrogens coupled to Cu(II) were identified in Cu(II)-Hc. Upon the binding of nitrite, a decrease in the hyperfine interaction for two of the three imidazole nitrogens was observed by ESEEM. Further, the results of a two-pulse ESEEM experiment are consistent with the assignment of the protons of a water ligand to Cu(II), which is displaced when nitrite is added. An analysis of X-ray absorption K-edge spectra suggests a coordination geometry intermediate between square-planar and tetrahedral for the metal centers in Cu(II)-Hc and Cu(II)-Hc-NO_2^-, in agreement with the g and A_{Cu} values determined by cw-EPR. On the basis of these results, an equivalent structure is suggested for Cu(II)-Hc-NO_2^- and the Cu(II) site in green half-methemocyanin, a partially oxidized binuclear derivative formed in the reaction of the native protein with nitrite.

Hemocyanin (Hc)[1] is a protein found in the hemolymph of mollusks and arthropods (Ellerton et al., 1983). Its physiological role is the reversible association of dioxygen at a binuclear copper active site. A complex currently formulated as Cu(II)−O_2^{2-}−Cu(II) is present in oxy-Hc, reflecting one-electron transfer from each cuprous copper of deoxy-Hc to the bound dioxygen (Van Holde et al., 1967; Brown et al., 1980).

The optical spectrum of oxy-Hc contains an intense band at 340 nm ($\epsilon \approx 20\,000$ M^{-1} cm^{-1}) arising from peroxide-to-Cu(II) and imidazole-to-Cu(II) ligand-to-metal charge-transfer transitions (Eickman et al., 1979). Another broad absorption band with a maximum at 570 nm ($\epsilon \approx 1000$ M^{-1} cm^{-1}) arises from a peroxide-to-Cu(II) charge-transfer transition and includes contributions in its red edge from Cu(II) d-d transitions (Eickman et al., 1979). The blue color of the protein is related to the presence of bound dioxygen, the deoxy and apo forms of the protein being colorless.

According to the three-dimensional structure of deoxy-Hc from *Panulirus interruptus (Arthropoda)*, determined to 3.2 Å resolution by X-ray crystallographic analysis of crystals formed at pH 4 (Linzen et al., 1985), each copper atom is coordinated to two nitrogen atoms from approximately coplanar histidyl imidazoles (Cu−N bond lengths = 2.0 Å) and, perpendicular to these, to a third histidine imidazole nitrogen at a distance of 2.7 Å. The Cu−Cu distance is 3.6 ± 0.4 Å. A second X-ray structure has been presented recently for subunit II of *Limulus polyphemus* deoxy-Hc, crystallized at pH 7 and high ionic strength (Hazes et al., 1993). In this Hc also, each copper is coordinated to three histidines, but here all are 2.0 ± 0.1 Å from the metal. The Cu−Cu distance is 4.5 Å in this case. The geometry of the active site for both crystallized proteins is approximately trigonal, and no evidence was found for a fourth ligand to copper (Linzen et al., 1985; Hazes et al., 1993).

The X-ray crystal structures of the deoxy-Hcs show that both metal atoms of the active site have similar coordination geometries, but one is more exposed to solvent (Linzen et al., 1985; Hazes et al., 1993). Accordingly, the kinetics of copper removal from holo-Hc by CN^- reveals a difference in the reaction rate for each of the two copper ions at the active site (Beltramini et al., 1984). It is therefore feasible to sequentially remove individual copper ions from a fast-reacting site (FRS) and a slow-reacting site (SRS), where this nomenclature is based on the relative rates of metal removal. Cyanide treatment also provides a means to prepare a stable apoprotein (Salvato et al., 1974), which is the starting material for the metal incorporation experiments described in this paper.

† This work was supported by CNR Grant 04.9312289 (B.S.) and NIH Grants GM 40168 and RR 02583 (J.P.).

* Author to whom correspondence should be addressed.

‡ Department of Physiology and Biophysics, Albert Einstein College of Medicine of Yeshiva University.

§ Department of Molecular Pharmacology, Albert Einstein College of Medicine of Yeshiva University.

|| University of Padua.

⊗ Abstract published in *Advance ACS Abstracts,* January 15, 1995.

[1] Abbreviations: Hc, hemocyanin; GHM, green half-met; NiR, nitrite reductase; FRS, fast-reacting site; SRS, slow-reacting site; cw, continuous wave; EPR, electron paramagnetic resonance; ESEEM, electron spin−echo envelope modulation; EXAFS, extended X-ray absorption fine structure; EDTA, ethylenediaminetetraacetic acid; XAS, X-ray absorption spectroscopy; Tris, tris(hydroxymethyl)aminomethane; TPP tetraphenylporphyrin; TEPA, tris[2-(2-pyridyl)ethyl]amine.

0006-2960/95/0434-1524$09.00/0

The preparation of a mononuclear Cu(II) derivative from apo-Hc is described. Several techniques were used in its characterization, including cw-EPR, ESEEM, and X-ray absorption spectroscopies. The rationale for its preparation is its use as a paramagnetic probe of the active site structure of the protein. Despite the presence of what is formally Cu(II) in oxy-Hc, this form is EPR silent due to antiferromagnetic coupling between the two Cu(II) ions mediated by bound dioxygen (Van Holde, 1967; Freedman et al., 1976). Furthermore, the oxidized, dicupric, met form of Hc, which does not bind O_2, is also EPR silent, implying the presence of a bridging ligand between the two metal ions that mediates a spin exchange interaction (Eickman et al., 1979).

One approach used in the past to obtain a paramagnetic center in the binuclear active site of Hc involves treatment of the holoprotein with nitrite to produce a Cu(I)−Cu(II) green half-met (GHM) derivative [Magliozzo et al. (1995) and references cited therein]. The structure of the active site in GHM is still under debate and is discussed in the preceding paper and will be addressed here. The insights obtained from spectroscopic analysis of the mononuclear Cu(II)-Hc derivative and its interaction with nitrite are relevant to structural and functional aspects of GHM Hc and to the enzyme nitrite reductase.[2]

MATERIALS AND METHODS

Carcinus maenas Hc was purified as previously described (Bubacco et al., 1992) from hemolymph collected by syringe from the dorsal lacunae of live animals. Samples of apo-Hc containing no native Hc and less than 5% of the copper content of holo-Hc were prepared from the holoprotein by dialysis against cyanide and EDTA (Salvato et al., 1974).

The monocopper derivative was prepared by dialyzing the apoprotein (2.5 mL, approximately 50 mg/mL) for 48 h at 20 °C against 500 mL of 0.1 M Tris−propionate, containing 125 μM $CuCl_2$ and 0.1% detergent (Tween 80, Aldrich), at pH 7.0. Excess reagents and unspecifically bound Cu(II) were then removed by dialysis against Tris−propionate containing 2 mM EDTA at pH 7. A similar procedure was followed using $^{65}Cu(NO_3)_2$ prepared from ^{65}CuO (ICON Services Inc., NJ).

Protein concentration was determined spectrophotometrically using $\epsilon_{278} = 9.3 \times 10^4$ M^{-1} cm^{-1} (Tamburro et al., 1977), where the extinction coefficient refers to a 75 kDa subunit. Optical absorption spectra were recorded on a Cary 14 spectrophotometer modified for computer control by Aviv Associates (Lakewood, NJ). The Cu(II)-to-protein molar ratios were obtained by relating the Cu(II) concentration in a sample (obtained by aromatic absorption) to the protein concentration evaluated optically.

Copper analysis was performed by atomic absorption spectroscopy using a Perkin-Elmer Model 5000 spectrophotometer equipped with a graphite furnace or an acetylene/air burner for flame analyses. A standard addition method was applied using atomic absorption standard copper solution (Aldrich) added to Hc samples containing approximately 5−10 μM protein. Fluorescence data were recorded at 20 °C using a Perkin-Elmer MPF 4 fluorimeter equipped with a thermostated cell compartment. Protein solutions used for fluorescence measurements had an optical absorbance of less than 0.06 at 295 nm, the excitation wavelength, to minimize inner filter effects (Lakowicz, 1986).

X-band continuous wave (cw) EPR spectra were recorded on a Varian E-112 spectrometer equipped with a Systron-Donner frequency counter and a Varian NMR Gaussmeter. Data collection and double integration of the signal intensities were executed using a personal computer interfaced to the EPR spectrometer and EPR data acquisition system programs provided by P. D. Morse (University of Illinois). For some samples, the copper concentration was determined by double integration of the EPR signal intensity for protein samples both before and subsequent to phosphoric acid treatment (1:1 dilution in 4% acid), using $CuSO_4 \cdot 5H_2O$ as a standard. EPR spectra of Cu(II)-Hc in the presence of different ligands were obtained by the addition of a small aliquot of a concentrated ligand solution to a ~1 mM protein sample, which was then frozen. cw-EPR spectral simulations were generated using the QPOWA program, supplied by L. Belford, as previously described (Nilges, 1979; Belford, 1981; Maurice, 1981).

Pulsed EPR studies were performed on a home-built spectrometer described in detail elsewhere (McCracken et al., 1987), using a strip-line transmission cavity (Mims, 1974) for ESEEM data collection. Both two-pulse (90°−τ−180°) and three-pulse (90°−τ−90°−T−90°) sequences were employed (Mims & Peisach, 1981). For the latter, the value of τ, the time interval between the first and second microwave pulses, was set as a multiple of the periodicity of the proton Larmor frequency in order to suppress modulations arising from weakly coupled protons (Mims & Peisach, 1981). In order to account for suppression effects, data were collected at different values of τ (Peisach et al., 1979; Mims & Peisach, 1979). To evaluate the intensity of the components contributing to the modulation function, data were collected at two different field positions in the $g_\perp$ region, where the intensity of the echo was maximal.

All ESEEM spectra are presented as Fourier cosine transforms of time domain data. Dead-time reconstruction and Fourier transformation of ESEEM data were performed as previously described (Mims, 1984). The details of the individual ESEEM experiments are reported in the figure legends. A density matrix formalism developed by Mims (1972) and angle-selection methods (Henderson et al., 1985; Hurst et al., 1985) were used for the simulation of experimental data.

Samples used for K-edge and EXAFS measurements were concentrated to about 2 mM by ultrafiltration using an Amicon Centricon microconcentrator, transferred to a Plexiglass sample holder, and frozen in liquid nitrogen. In order to monitor the condition of samples after X-ray exposure, EPR spectra were collected after dilution in buffer. No significant differences were observed between the EPR spectra of the derivatives collected before and after the EXAFS experiments.

XAS measurements were conducted at the National Synchrotron Light Source, Brookhaven National Laboratory (Upton, NY) (beam line X10C, flux = 1.0×10^{10} photons s^{-1} cm^{-2} at 100 mA beam current). Kα copper fluorescence data were collected using a 13-element solid state germanium detector. A transmission experiment was simultaneously carried out on copper foil in order to obtain an energy calibration for each fluorescence scan. The temperature of

[2] A class of diheme (c, d_1) containing NiRs has been also described (Hochstein & Tomlinson, 1988); however, in our study only the copper enzyme will be considered.

the system was maintained at about 130 K with a cryostat (Powers et al., 1982).

K-edge and EXAFS data were analyzed as described previously (Lee et al., 1981; Powers et al., 1982). Single scans were inspected for the presence of irregularities and were rejected if sudden changes in signal or beam intensity were detected. Three K-edge scans per sample and four EXAFS scans per sample were averaged prior to analysis in order to improve the signal-to-noise ratio. The free atom contribution to the EXAFS data was subtracted by using a cubic B-spline, and the data were multiplied by k^3 in order to compensate for the k^{-3} dependence assumed at high values of k. The background-subtracted data, weighted for k^3, were Fourier transformed (K range 12 $Å^{-1}$) and then back transformed. First-shell contributions were isolated with a Fourier filter using a square window function. The Fourier-filtered data were back transformed and then fit using data for model complexes with versions of the AT&T Bell Laboratories EXAFS programs modified for personal computer (Scheuring et al., 1994).

Two approaches were used in the iterated fitting procedures. In one, distances, coordination number (N), ΔE (difference in threshold energy between the sample and the model data), and the Debye−Waller factor (relative to the model complex, solid CuTPP) were allowed to vary independently. In the second, the number of ligands was fixed (the value was increased stepwise from a minimum of two to a maximum of six ligands), and all of the other parameters were allowed to vary. Both approaches gave similar final fit parameters. The error in the determination of bond lengths and number of ligands was determined as the difference in these values that produces a 2-fold increase in the value of χ^2 (sum of residuals squared) for the fitting of the first coordination shell (Lytle et al., 1989).

RESULTS

Preparation of Cu(II)-Hc. The preparation of this mononuclear copper derivative of Hc was accomplished by a 24 h dialysis of apoprotein against buffer containing Cu(II) and Tris−propionate.[3] The Cu(II)-containing derivative was purified by dialysis against EDTA in order to remove excess reagents and nonspecifically bound Cu(II). The formation of the derivative was monitored by evaluation of the tryptophan fluorescence quenching upon Cu(II) binding to the apoprotein and by the stoichiometry of EDTA-resistant Cu(II) bound to the protein, as determined by both atomic absorption spectroscopy and double integration of EPR signal intensity. The EPR absorption intensity due to Cu(II) did not increase in a sample of Cu(II)-Hc subsequent to protein denaturation in phosphoric acid, indicating that all copper bound to the mononuclear site was EPR active (data not shown).

The fluorescence of Hc (λ_{max} = 330 nm) upon excitation at 295 nm arises from several tryptophans (Bannister & Wood, 1971). The difference in the fluorescence intensity

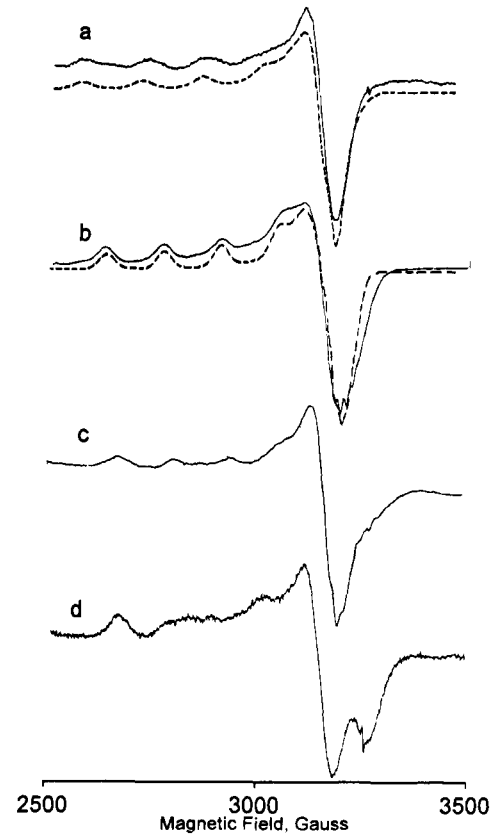

FIGURE 1: cw-EPR spectra: (a) spectrum of Cu(II)-Hc in 20 mM phosphate buffer (pH 7) (the dotted line is the simulated spectrum; see Table 1; (b) spectrum of Cu(II)-Hc in 100-fold excess nitrite (the dotted line is the simulated spectrum; see Table 1); (c) spectrum of Cu(II)-Hc plus 6-fold excess CN^-; (d) spectrum of Cu(II)-Hc plus 10-fold excess N_3^-. Spectrometer conditions: (a) microwave frequency, 9.108 GHz, microwave power, 2 mW, modulation amplitude, 5 G; (b) microwave frequency, 9.106 GHz; (c) microwave frequency, 9.108 GHz; (d) microwave frequency, 9.12 GHz.

observed for apo- and deoxy-Hc is believed to derive for the most part from the quenching of a specific tryptophan fluorescence due to the metal ion bound nearby in the active site (Bannister & Wood, 1971; Salvato et al., 1986). X-ray crystallographic analysis shows that the closest contact with Trp 197 in *P. interruptus* Hc (a member of the Decapoda order, like *C. maenas*) is about 9 Å from one of the copper ions, Cu_A, in the active site (Linzen et al., 1985). The binding of a single Cu(II) to *C. maenas* apo-Hc produces a 40% decrease in the fluorescence quantum yield to a value close to that observed for deoxy-Hc (data not shown). This result suggests that, in Cu(II)-Hc, the copper ion is bound in the Cu_A site.

Optical Spectroscopy of Cu(II)-Hc. The optical absorption spectrum of Cu(II)-Hc in the visible region shows the characteristic low-intensity d-d transition patterns due to Cu(II) (λ_{max} = 650 nm, $\epsilon \cong 60\ M^{-1}\ cm^{-1}$), which gives the derivative a pale green color. The absence of absorptions at 340 and 570 nm indicates that no oxyprotein was present in the samples used in these studies.

cw-EPR Spectroscopy of Cu(II)-Hc. The cw-EPR spectrum of Cu(II)-Hc (Figure 1a) is typical of a $d_{(x^2-y^2)}$ ground state site and could be adequately simulated by assuming axial symmetry (Table 1). Upon the addition of a 100-fold molar excess of nitrite, significant changes in the shape of the spectrum were observed (Figure 1b). On the basis of spectral simulation, a small difference between g_x and g_y was

[3] With longer incubation times, the reaction proceeds to reconstitute a small fraction of binuclear sites (≈5%) as indicated by the appearance of an LMCT at 350 nm, typical of the oxygenated protein. In order to bind oxygen, the copper ions in the binuclear site must be in the cuprous state. A possible reductant in this system could be CN^- present as a contaminant retained in the preparation of the apoprotein (Witters et al., 1982).

Table 1: Parameters Obtained by Simulation of cw-EPR Spectra

derivative	g_x	g_y	g_z	A_x[a] (MHz)	A_y (MHz)	A_z (MHz)
Cu(II)-Hc	2.065	2.065	2.320	20	20	450
Cu(II)-Hc-NO_2^- [b]	2.045	2.055	2.290	40	40	415
GHM Hc[c]	2.049	2.095	2.295	40	40	410
NiR[d]	2.065[e]	2.065	2.342	*f*	*f*	368
NiR[g]	2.045[h]	2.045	2.355	*f*	*f*	366

[a] A_x and A_y for Cu(II) are not resolved in the cw-EPR spectra, and these terms only contribute some line width at g_x and g_y, the remainder of which is incorporated using Lorenztian line-broadening terms of similar magnitude (40 MHz). The program QPOWA was used for all simulations (see Materials and Methods). [b] 100-fold excess nitrite. [c] GHM, green half-met-Hc from *C. maenas* (Magliozzo et al., 1995). [d] Nitrite reductase from *A. cycloclastes*. [e] Libby & Averill, 1992. [f] These values were not reported. [g] Nitrite reductase from *Alcaligenes xylosoxidans*. [h] Howes et al., 1994.

evaluated (Table 1), due to rhombic distortion of the coordination geometry. Furthermore, a decrease in $A_{||}$ was observed. Superhyperfine features (~14 G splitting) likely to arise from directly coordinated ^{14}N were resolved in the $g_\perp$ region of the spectrum of Cu(II)-Hc-NO_2^-. Seven equally spaced lines were resolved, suggesting multiple nitrogen coordination. The same features were also observed in an isotopically homogeneous (100% ^{65}Cu) sample, supporting the assignment suggested earlier for the origin of the splitting.

Upon the removal of excess nitrite by extensive dialysis of Cu(II)-Hc-NO_2^-, the EPR spectrum of the original sample observed before nitrite addition was obtained, demonstrating that nitrite reversibly binds to Cu(II)-Hc. In order to rule out a simple ionic strength effect as the source of the perturbation of the cw-EPR spectrum, 100-fold excess nitrate instead of nitrite was added to Cu(II)-Hc. No detectable difference was observed in the EPR spectrum (data not shown).

Cyanide binding also gave a rhombic EPR spectrum (Figure 1c). Furthermore, with cyanide a poorly resolved superhyperfine structure appeared in the $g_\perp$ region. For this derivative, cyanide binding to Cu(II) was substantiated by the increased broadening of the $A_{||}$ features in the complex prepared with $^{13}CN^-$ (data not shown). The effect of azide was also investigated (Figure 1d). Here, a significant effect on the line shape of the EPR spectrum was noted, indicative of a larger rhombic distortion than that obtained with nitrite.

ESEEM MEASUREMENTS

Three-Pulse ESEEM. ESEEM arises from weak magnetic coupling between the electron spin of Cu(II) and its surrounding nuclei (Mims & Peisach, 1981). The ESEEM spectrum of Cu(II)-Hc is shown in Figure 2a. It is known from the available X-ray structures that the copper ligands provided by the protein matrix in Hcs are the N_ϵ of histidyl imidazoles (Linzen et al., 1985; Hazes et al., 1993). The coupling of these directly coordinated nitrogens, however, is too large to give rise to envelope modulation (Mims & Peisach, 1978). Therefore, the observed ESEEM is generated by the coupling between the Cu(II) ion and the remote nitrogens of the coordinating imidazoles.

An assignment of the many lines observed in the Fourier transform of the three-pulse ESEEM data can be accomplished according to a spin Hamiltonian for ^{14}N described

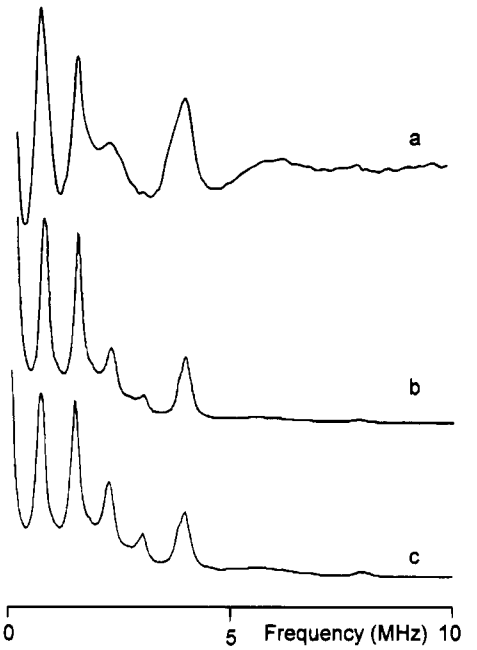

FIGURE 2: Three-pulse ESEEM spectrum for Cu(II)-Hc and spectral simulations. The values for parameters used in the simulations are listed in Table 2: (a) Cu(II)-Hc in 20 mM phosphate buffer (pH 7); (b) spectral simulation obtained by assuming the contribution of two equivalent nitrogens; (c) spectral simulation obtained by assuming the contribution of three equivalent nitrogens. Experimental conditions: (a) microwave frequency, 9.123 GHz; g = 2.0694; τ = 223 ns; magnetic field, 3150 G.

elsewhere [Jiang et al. (1990) and references cited therein]:

$$H_N = -g_N\beta_N\mathbf{HI} + \mathbf{SA}_N\mathbf{I} + h\mathbf{IQI}$$

The first term in the Hamiltonian is the nuclear Zeeman interaction defined by the nuclear g factor (g_N), the Bohr magneton (β_N), the external magnetic field (**H**), and the nuclear spin operator (**I**). The second term, the electron–nuclear superhyperfine interaction, is defined by the electron spin operator (**S**), the superhyperfine tensor ($\mathbf{A}_N$), and **I**. At the frequency and field used to collect the ESEEM data (X-band), the nuclear Zeeman and the electron–nuclear superhyperfine interactions contributing to the spin Hamiltonian almost cancel each other in one of the ^{14}N submanifolds and add in the other (Mims & Peisach, 1978). The first case defines the exact cancellation condition (Flanagan & Singel, 1987), where only the third term in the spin Hamiltonian contributes to the splitting of the energy levels. This term describes the nuclear quadrupole interaction (NQI) (where h is Plank's constant and **Q** is the quadrupole interaction tensor). The splitting of the energy levels in the submanifold only defined by the NQI gives rise to three sharp lines in the low-frequency region of the ESEEM spectrum, where the value of the higher frequency line corresponds to the sum of the two lower frequency ones (Mims & Peisach, 1978).

In the spectrum of Cu(II)-Hc (Figure 2a), the two lower frequency lines coincide, appearing as a single line at 0.73 MHz, and the third component is observed at around double this frequency, 1.54 MHz. The submanifold where the nuclear Zeeman and the electron–nuclear hyperfine interactions sum gives rise to only one broad line (at 3.92 MHz in Figure 2a), which arises from a double-quantum transition. The two other single-quantum transitions of this submanifold

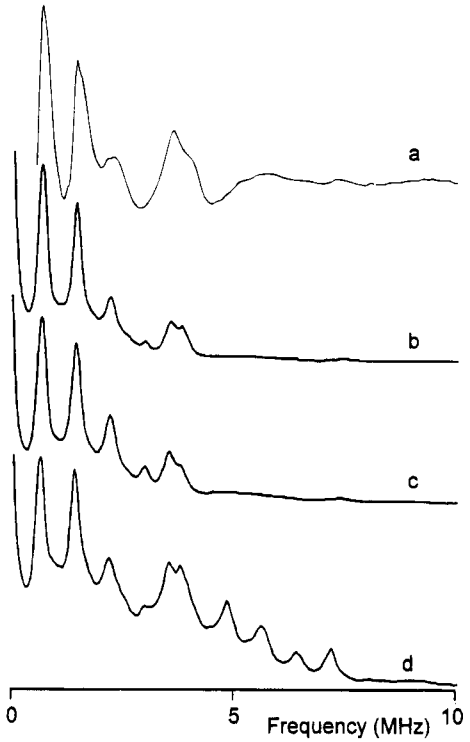

FIGURE 3: Three-pulse ESEEM spectrum for Cu(II)-Hc-NO_2^- and spectral simulations. The values for parameters used in the simulations are listed in Table 2: (a) Cu(II)-Hc in 100-fold excess nitrite; (b) spectral simulation obtained by assuming the contribution of two nitrogens (A_{ISO}(N1) = 1.45 MHz, A_{ISO}(N2) = 1.75 MHz); (c) spectral simulation obtained by assuming the contribution of three nitrogens (A_{ISO}(N1,N2) = 1.45 MHz, A_{ISO}(N3) = 1.75 MHz); (d) same simulation as for spectrum c plus the contribution of an equatorially bound nitrite molecule (see Table 2 and text for explanations). Experimental conditions: (a) microwave frequency, 9.119 GHz; g = 2.136; τ = 223 ns; magnetic field, 3050 G.

are not observed because of broadening due to their strong angular dependence (Mims & Peisach, 1978). The low-intensity peaks observed at 2.23 and 3.0 MHz and at about 7.44 MHz (about 2 times the frequency of the double-quantum transition) are combination lines indicating that several nuclei having similar interactions with the electron spin are bound to copper (Lin et al., 1986; McCracken et al., 1989). For multiple nitrogen coordination, as in this case, the function that describes the modulation of the echo intensity is the product of the modulation function of each of the nuclei considered separately (Lin et al., 1986; McCracken et al., 1989).

The Fourier transform of the three-pulse data for Cu(II)-Hc-NO_2^- (Figure 3a) shows the same features described earlier, with small differences in the frequencies of the NQI lines and partial resolution of two double-quantum transitions. The implication of these new features will be considered in the following.

Three-Pulse Data Simulation. The simulation procedure and the contributions of the individual parameters to the calculated spectra are described and discussed in detail elsewhere (Magliozzo & Peisach, 1992). Table 2 summarizes the values used to generate the spectral simulations presented in Figure 2c and Figure 3c,d. The NQI parameters for both Cu(II)-Hc and the nitrite adduct are typical for imidazole δ-nitrogens forming strong hydrogen bonds with either the protein matrix or water (Jiang et al., 1990). This observation is consistent with the X-ray structure of *L. polyphemus* Hc, where all of the remote nitrogens of the Cu-coordinated imidazoles are hydrogen bonded (Hazes et al., 1993).

Table 2: Nitrogen Nuclear Hyperfine and Quadrupole Coupling Parameters Obtained by Simulation of ESEEM Spectra[a]

derivative	N^b	A_x	A_y	A_z	A_{ISO}^c	e^2Qq	η^c
Cu(II)-Hc	3	1.44	1.9	1.88	1.74	1.52	0.92
		(0, 70, 0)[d]				(0, 40, 0)	
Cu(II)-Hc-NO_2^-	2	1.24	1.56	1.56	1.45	1.50	0.88
		(0, 70, 0)[d]				(0, 40, 0)	
	1	1.45	1.90	1.90	1.75	1.50	0.90
		(0, 70, 0)[d]				(0, 40, 0)	
Cu(II)-TEPA-NO_2^- [e]	1	3.4	3.4	3.4	3.4	5.66	0.32
						(20, 90, 0)	

[a] The estimated errors in the value of A_{ISO}, e^2Qq, η, and Euler angles are 10%. [b] Number of $^{14}N_\delta$ assumed to contribute to the modulation function. [c] A_{ISO} is calculated as $(A_x + A_y + A_z)/3$. $\eta = (q_{xx} - q_{yy})/q_{zz}$. [d] Euler angles (in degrees) α, β, and γ relative to the principal axes of the **g** tensor. [e] Jiang et al., 1993.

In the ESEEM spectra of Cu(II)-Hc, the line shape of the double-quantum transition suggests the presence of a single class of equivalent nitrogens. The hyperfine coupling, A_{ISO} = 1.73 MHz,[4] was evaluated by spectral simulation.

Upon addition of nitrite, the splitting of the $\Delta m_I = 2$ transition is the only substantial change observed in the spectrum. This effect was reproduced in a simulation by assuming that a weaker and a stronger coupling interaction were present. A new set of parameters was applied in the simulation to reproduce the line shape of the double-quantum transitions for both classes of ^{14}N. Then, the individual modulation functions, weighted by the integer number of nitrogens of that class, were multiplied to produce the simulated spectrum. The best fit was obtained by assuming the contribution of two nitrogens with A_{ISO} = 1.45 MHz and one with A_{ISO} = 1.74 MHz (Figure 3c). The values obtained from the simulation of the data collected at 3050 G were verified by an analogous simulation of data collected at 3150 G (data not shown).

In order to investigate the potential contribution to the modulation function from the nitrogen of bound nitrite, a simulation was carried out that included the coupling parameters for three imidazole δ-nitrogens, as well as those assumed for the nitrogen of a nitrite ligand. The ^{14}N nitrite parameters used in the simulation (Table 2) were taken from those reported for Cu(II)-TEPA-NO_2^- (Jiang et al., 1993). In this complex, the nitrite is bound to copper as an equatorial ligand, via an oxygen atom. The sharp peak at about 4.9 MHz, observed in the simulation (Figure 3d) and attributed to the sum of the two lower frequency NQI lines of ^{14}N of nitrite, is not observed in the ESEEM data for the nitrite derivative of Cu(II)-Hc (Figure 3a). Furthermore, a double-quantum transition at 7.1 MHz expected for nitrite and the combination lines derived from the 4.9 MHz line and the imidazole NQI lines are present in a region of the simulation where no feature is observed in the data. These observations suggest that, in Cu(II)-Hc-NO_2^-, the nitrogen hyperfine coupling for $^{14}NO_2^-$ is not similar to the value reported for an equatorial ligand in the model.

Since the presence of combination lines in the ESEEM spectra suggests that more than one nitrogen is coordinated to the copper ion, an attempt was made to evaluate their

[4] The value of A_{ISO} is calculated as $(A_x + A_y + A_z)/3$.

number for Cu(II)-Hc and Cu(II)-Hc-NO_2^-. Two cases were explored in simulations. In one, the spectrum was assumed to contain the contributions of only two δ-nitrogens, as suggested from the X-ray structure of *P. interruptus* Hc, where two of the three directly coordinated ϵ-nitrogens are about 2.0 Å from the Cu(II)[5] (all equivalent, shown in Figure 2b; one with a strong and one with a weak coupling, shown in Figure 3b). A second case was explored where three δ-nitrogens (all equivalent, shown in Figure 2c; two with a strong and one with a weak coupling, shown in Figure 3c) were assumed to contribute to the modulation function, as suggested by the X-ray structure of *L. polyphemus* Hc. Here, the three coordinating ϵ-nitrogens are all about 2.0 ± 0.1 Å from the copper ion.

A number of tests were applied to evaluate the spectral features in data and in simulations. For example, the best fits of the intensities of the combination lines at 2.3 and 3 MHz relative to the quadrupole lines were obtained by assuming a contribution of only two nitrogens (Figures 2b and 3b). However, the relative intensities of the combination lines in the data for Cu(II)-Hc were comparable to the published ESEEM spectra for two Cu(II)−imidazole complexes, $Tr(His)_3$ and its analogue $Ar(His)_3$ (Goldfarb et al., 1991), where three imidazoles are known to be coordinated to Cu(II). One may conclude that the intensities of the combination lines in a simulation are somewhat higher than those in experimental data for complexes containing multiple nitrogen coordination. Thus, on the basis of the intensities of the combination lines alone, two is probably an underestimate of the real number of coupled nitrogens in Cu(II)-Hc.

Another approach to quantitate imidazole ligands was based on the intensity and line shape of the double-quantum lines compared to the intensity of the NQI lines. Also in this case, the spectral simulations, especially for Cu(II)-Hc-NO_2^- (Figure 3b,c), suggest the contribution of three ^{14}N to the modulation function for Cu(II)-Hc. This approach is described in more detail in Magliozzo et al. (1995).

Two-Pulse ESEEM. Two-pulse ESEEM data for Cu(II)-Hc and its nitrite complex were obtained to examine the electron−nuclear coupling due to protons near Cu(II). In the frequency range 0−10 MHz, a complex pattern of lines is observed representing fundamental, sum, and difference frequencies attributed to electron−nuclear coupling to ^{14}N and ^1H (Figure 4a). Low-intensity peaks between 10 and 30 MHz, which exhibit the same pattern in the spectra of Cu(II)-Hc with and without nitrite, are assigned to sum and difference components for all coupled nuclei (Figure 4b,c). In the region at higher frequency, lines are observed near the proton Larmor frequency and at twice that value. The positive peak at 13.4 MHz and a negative peak at 26.8 MHz are assigned to the first (ν_I) and second ($2\nu_I$) harmonics of the proton Larmor frequency at 3150 G, the field strength at which the data were collected. These two features are assigned to solvent molecules and to other protons that are close enough to the Cu(II) to be magnetically coupled, but are not coupled strongly enough to have a coupling frequency shifted from the Larmor frequency.

[5] The coupling from the δ-nitrogen of the third imidazole is ignored as the Cu ϵ-nitrogen distance is 2.7 Å. The magnitudes of coupling for the directly coordinated and for the remote nitrogens will make little contribution to the modulation (Cornelius et al., 1990).

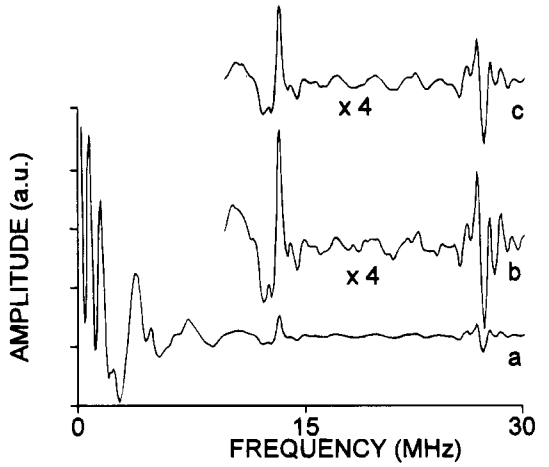

FIGURE 4: Two-pulse ESEEM spectra: (a) Cu(II)-Hc-NO_2^-; (b) Cu(II)-Hc in 20 mM phosphate buffer (pH 7); (c) Cu(II)-Hc-NO_2^-. Parameters: (a) microwave frequency, 9.123 GHz; g = 2.069, magnetic field, 3050 G.

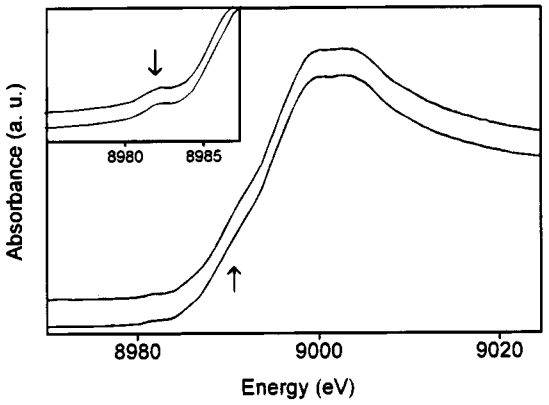

FIGURE 5: X-ray absorption K-edge spectra of Cu(II)-Hc in 20 mM phosphate bufffer (pH 7) (bottom spectrum) and Cu(II)-Hc-NO_2^- (top spectrum). The arrows indicate the 1s → 4p plus shake-down transition and the 1s → 3d transition (inset).

More tightly coupled protons contribute an additional feature to the Cu(II)-Hc spectrum, appearing as a negative peak at 0.75 MHz to higher frequency of $2\nu_I$ (Figure 4b). This feature corresponds to a sum combination peak (Mims et al., 1977). In a d_{z^2} nickel cyanide complex, an analogous feature has been assigned to the H of axially bound water (McCracken & Friedenberg, 1994). Similarly, in an ESEEM study of $Cu(H_2O)_6^{2+}$, two features shifted by 0.57 and 1.14 MHz from the second harmonic of the proton Larmor frequency are observed (Schweiger, 1989) and are assigned to protons of axially and equatorially coordinated water, respectively. The magnitude of the observed shift for Cu(II)-Hc is in line with a proton from a water molecule axially bound to Cu(II). For the spectrum of Cu(II)-Hc-NO_2^-, there is a decrease in the intensity of the feature at $2\nu_I$ + 0.75 MHz compared to that for Cu(II)-Hc. This reduction suggests that protons (likely from H_2O) contributing to this feature are displaced by nitrite.

XAS MEASUREMENTS

K-Edge. In Figure 5, the K-edge spectra of Cu(II)-Hc and Cu(II)-Hc-NO_2^- are shown. The two spectra, after normalization of the edge jump, are almost equivalent. Two features are of interest, the low-intensity preedge peak at 8982 eV (inset in Figure 5) and the shoulder at about 8993 eV (Figure

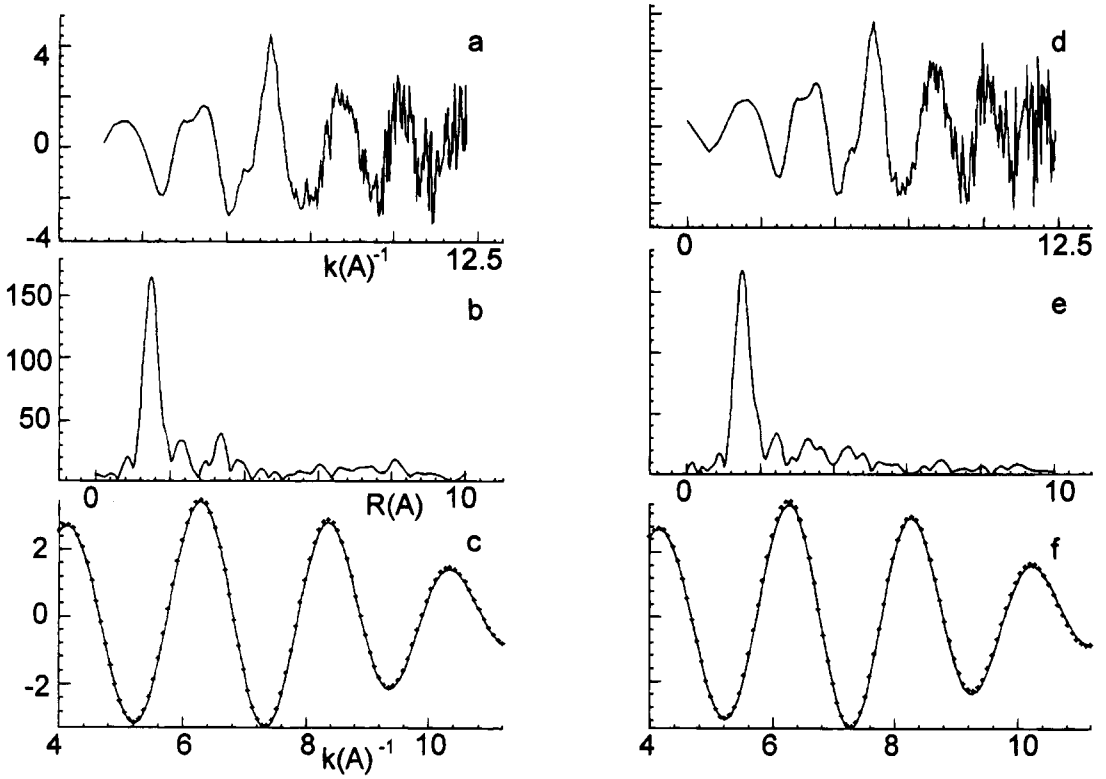

FIGURE 6: EXAFS data: (a) Cu(II)-Hc raw data; (b) Fourier transform of Cu(II)-Hc data; (c) back-transform data for the first coordination shell of Cu(II)-Hc (points, experimental data; continuous line, fitting (see Table 3 for fitting parameters); (d) Cu(II)-Hc-NO_2^- raw data; (e) Fourier transform of Cu(II)-Hc-NO_2^- data; (f) back-transform data for the first coordination shell of Cu(II)-Hc-NO_2^- (points, experimental data; continuous line, fitting (see Table 3 for fitting parameters)).

5). The former is assigned to a 1s → 3d transition, and the presence of this feature is usually indicative of tetrahedral coordination geometry for Cu(II) in small molecule complexes (Sano et al., 1992). Furthermore, the intensity of this transition has been correlated with the dihedral angle between the two planes defined by the metal and each of the two ligand pairs in four-coordinate complexes (Sano et al., 1992). The similarity in the 1s → 3d transition intensities for Cu(II)-Hc and the nitrite complex suggests that no change in the structure occurs when nitrite is bound. Small rearrangements cannot be ruled out since a significant change in intensity of the feature has been noted only for rather large changes in dihedral angles (Sano et al., 1992).

The second feature at 8993 eV has previously been assigned to a 1s → 4p plus shake-down transition for square-planar complexes (Kosugi et al., 1984; Smith et al., 1985). In the study by Sano et al. (1992), the intensity of this peak, which is well resolved in a square-planar complex, decreases with increasing dihedral angles and is absent when the coordination geometry of the metal complex is close to tetrahedral. Therefore, the presence of both a weak 1s → 4p transition plus shake-down and the 1s → 3d transition indicates a distorted four-coordinate geometry for Cu(II) in both Cu(II)-Hc and Cu(II)-Hc-NO_2^-.

EXAFS Analysis. In the analysis of the first coordination shell, χ^2 and the Debye–Waller factor were evaluated as a function of bond length and coordination number (the latter being increased stepwise from a minimum of two to a maximum of six ligands). The best fit for the first coordination shell of Cu(II)-Hc was obtained by assuming three ligands (N, O type) at 1.99 ± 0.01 Å and one (N, O type) at 2.22 ± 0.01 Å (Figure 6c and Table 3). An analogous result was obtained in fitting the Cu(II)-Hc-NO_2^- data (Figure 6f and Table 3). This suggests that nitrite binding occurs with no change in coordination number. It is worthwhile to point out that, in the Fourier transform for both Cu(II)-Hc and its nitrite derivative, a peak at $r \approx 3$ Å, generally assigned to the scattering of a second metal in the outer shell of the binuclear site of Hc (Woolery et al., 1984), is absent, substantiating the assumption that Cu(II)-Hc is mononuclear. Furthermore, the Fourier transforms show small differences between Cu(II)-Hc and Cu(II)-Hc-NO_2^- in the outer shell region (Figure 6b,e). Such differences could be due to the presence of a different ligand in the two derivatives or to a rearrangement of the ligand imidazoles. However, no attempt was made to fit the outer shell data.

Table 3: Parameters Used in the Fit of the EXAFS Data for the First Coordination Sphere Ligands

derivative	R^a (Å)	N^b	$\Delta\delta^2 \times 10^{-3}$ ^{c}	ΔE^d	χ^2 ^{e}
Cu(II)-Hc	1.97	4	5.48	3.6	15.61
	1.96	3	−2.64	3.25	2.38
	1.98	3	2.17	1.2	0.29
	2.22	1	−13.6	5.78	
	1.98	3	2.28	1.86	0.26
	2.22	0.65	−8.7	5.91	
Cu(II)-Hc-NO_2^-	1.97	4	−5.08	1.06	17.40
	1.97	3	−2.28	0.73	2.78
	1.97	3	1.79	0.67	0.28
	2.21	1	17.8	2.43	
	1.97	3	−1.79	0.15	0.23
	2.21	0.5	−8.7	2.95	

^{a} Cu–L distance ± 0.02 Å. ^{b} Number of scatterers (N,O type). ^{c} Debye–Waller factor. ^{d} Threshold energy difference between the model and the experimental data. ^{e} Square of the residuals between model and fit.

DISCUSSION

A mononuclear derivative of *C. maenas* Hc, prepared from reaction of the apoprotein and Cu(II) in the presence of propionate, has been isolated. The 1:1 stoichiometry of EDTA-resistant Cu(II) bound per protein subunit is demonstrated by atomic absorption and EPR spectroscopies. The derivative does not contain EPR silent met sites (Cu(II)-Cu(II)) nor cuprous sites as no increase in EPR signal intensity occurs upon acid denaturation. The absence of a ligand-to-metal charge-transfer transition at 340 nm, characteristic of oxy-Hc (Van Holde et al., 1967; Brown et al., 1980), also indicates that no dicuprous sites are present.

It is known that the fluorescence of a tryptophan, conserved in many Hcs (Trp 197 in *P. interruptus* Hc) (Linzen et al., 1985), is quenched when copper is bound in the FRS and is not affected by the presence of a metal ion in the SRS (Beltramini et al., 1984). As only a single copper ion is bound to Cu(II)-Hc, the observed fluorescence quenching of Trp suggests that it is likely to be bound at the FRS.

The cw-EPR spectrum of Cu(II)-Hc is consistent with a $d_{(x^2-y^2)}$ ground state (Abragam & Bleaney, 1970). Although three equivalently coupled imidazoles are shown to be coordinated to the Cu(II) by ESEEM spectroscopy, there are no resolved ^{14}N superhyperfine features in the cw-EPR spectrum. The line widths of the $A_{||}$ features suggest that ligand heterogeneity (OH^- or H_2O) could account for the absence of resolved superhyperfine structure.

Complementary information on the coordination number and geometry of copper has been obtained by X-ray absorption spectroscopy. The fitting of EXAFS data for the first coordination shell of Cu(II) in Cu(II)-Hc indicates the presence of three ligands (N or O) 1.98 ± 0.01 Å and a fourth ligand 2.22 ± 0.01 Å from the copper. Similarly, three equivalent δ-nitrogens of imidazole are detected in three-pulse ESEEM experiments. Therefore, it is reasonable to assign the three ligands found by EXAFS at a shorter distance to the directly coordinated ϵ-nitrogens of imidazoles. The identification of the fourth ligand in Cu(II)-Hc is based on two-pulse ESEEM spectra. More precisely, the presence of a peak shifted 0.75 MHz from the second harmonic of the proton Larmor frequency in the Fourier transform indicates a hyperfine interaction with protons, consistent with a water molecule (or OH^-) bound to the copper ion.

The geometry of coordination of the metal site in Cu(II)-Hc, as suggested by the K-edge data analysis, is between square planar and tetrahedral. Also consistent with this assignment are the g and $A_{||}$ values obtained from simulation of the cw-EPR spectrum, although these are closer to the values expected for square-planar copper with N and O ligands (Peisach & Blumberg, 1974).

The binding of nitrite to Cu(II)-Hc is demonstrated by the change in line shape of the cw-EPR spectrum. One such change is the appearance of seven equally spaced superhyperfine features in the $g_\perp$ region, which suggests coupling from multiple directly coordinated nitrogens. This finding is consistent with the assignment based on the simulation of three-pulse ESEEM data, in which the contribution of three remote imidazole nitrogens was identified. Furthermore, the presence of two partially resolved double-quantum-transition lines in the ESEEM spectra of Cu(II)-Hc-NO_2^- indicates two classes of coupling. The addition of nitrite restructures the Cu(II) site so that there is a reduction of the electron−nuclear coupling to two of the three imidazole nitrogens. This nonequivalence is not resolved by EXAFS of Cu(II)-Hc-NO_2^-, for which the best fit is obtained by assuming three equivalent close ligands plus a fourth one at a longer distance.

It is interesting to note that no change in coordination number occurs when nitrite binds, demonstrating that the reaction is a ligand displacement. Since the three-pulse ESEEM of Cu(II)-Hc-NO_2^- suggests that none of the nitrogen ligands from the protein are displaced by nitrite binding, the fourth ligand (2.2 Å from the copper), detected by EXAFS and earlier suggested to be a water molecule, is the one that is exchanged. The observed reduction in intensity of the $2\nu_I$ + 0.75 MHz peak in the two-pulse ESEEM measurement when nitrite binds is also consistent with the proposed structure. The binding of azide or cyanide is also likely to occur as a displacement of the water ligand.

The ligand structure suggested here for Cu(II)-Hc is analogous to that of the type 2 site in nitrite reductase (NiR) from *Achromobacter cycloclastes* determined by X-ray crystallography (Godden et al., 1991). In NiR, three imidazole ϵ-nitrogens, which form a plane approximately 0.3 Å below the copper atom, and a water molecule coordinate the metal in a distorted tetrahedral site. The EPR parameters of this site in NiR (Table 1) are close to those for Cu(II)-Hc, although a lower value for $A_{||}$ indicates a more tetrahedral structure for NiR.

Another analogy that can be drawn is between the ligand exchange chemistry of Cu(II)-Hc and NiR. The first indication of the structural rearrangement that occurs upon substrate binding to NiR was obtained from a comparison of X-ray diffraction data collected for isomorphous protein crystals with and without nitrite (Libby & Averill, 1992). This study suggested that the coordinated water molecule in the type 2 site was exchanged with nitrite. The two-pulse ESEEM study of Cu(II)-Hc suggested a similar exchange reaction.

A binuclear derivative of Hc that shares many of the physical properties of the nitrite complex of Cu(II)-Hc is the GHM derivative prepared by treatment of native Hc with nitrite [Magliozzo et al. (1995) and references cited therein]. In this derivative, one of the copper atoms of the binuclear site is cupric and the other is cuprous. The similarities in the EPR, ESEEM, and optical properties lend support to the view that the nitrite complexes of Cu(II)-Hc and Cu(II) in GHM Hc have similar structures. EXAFS of Cu(II)-Hc in both the presence and absence of nitrite indicates a tetracoordinate structure. A similar coordinatin for the Cu(II) site in the binuclear GHM Hc is proposed in the preceding paper (Magliozzo et al., 1995).[6]

Although nitrite binding to Cu(II) in GHM Hc has been suggested, EPR (Van der Deen & Hoving, 1977) and ESEEM (Jiang et al., 1993) studies on GHM Hc have not elucidated a coupling interaction between Cu(II) and the nitrogen of $^{14}NO_2^-$ or $^{15}NO_2^-$. According to an ESEEM study on a model compound with square-pyramidal geometry (Cu(II)-TEPA-NO_2^-), the ^{14}N hyperfine interaction for an equatorial nitrite bound via oxygen (Cu−O distance = 2.04

[6] An EXAFS analysis of the GHM Hc derivative is hindered by the presence of the second copper in the binuclear site, which does not allow an unambiguous determination of the coordination number for the cupric copper. It therefore was not undertaken.

Å) is 3.4 MHz or about 1 G (Jiang et al., 1993). A spectral feature attributed to such a small magnetic coupling would not be resolved in a cw-EPR spectrum for Cu(II). The phenomena responsible for the absence of a contribution from the bound ^{14}N of nitrite to the ESEEM spectrum of Cu(II)-Hc-NO_2^- are not yet understood. The contributions from the nitrite to the ESEEM spectrum of the model we have examined are very shallow relative to the imidazole contribution in the Hc case. The structural differences between Cu(II)-TEPA-NO_2^- and Cu(II)-Hc-NO_2^- are a departure from an equatorial position of the nitrite ligand and an increased separation between Cu(II) and ^{14}N [Cu−O distance is 2.21 Å for Cu(II)-Hc-NO_2^- (Table 3)] for the latter. These structural differences may lead to changes in coupling that result in a more shallow or undetectable contribution from the bound nitrite. Furthermore, in the case of nitrite reductase, no difference was observed in the ENDOR spectra of $^{15}NO_2^-$- and $^{14}NO_2^-$-bound forms of the protein (Howes et al., 1994), suggesting that the coupling to nitrogen in this ligand is much reduced in nontetragonal coordination geometries.

Contrary to what was observed for GHM Hc [Magliozzo et al. (1995) and references cited therein], nitrite bound to Cu(II)-Hc can be removed by simple dialysis. This reversible binding of nitrite was also observed by Himmelwright et al. (1978) in the met-apo mononuclear derivative from *Busycon canaliculatum* Hc, prepared by partial copper depletion with CN^-, followed by oxidation of the remaining bound copper. The reversibility of nitrite binding to met-apo-Hc from *B. canaliculatum* led to the suggestion that, in the binuclear green half-met-Hc derivative, Cu(I) is involved in the formation of a bridge that is responsible for the high affinity of the exogenous ligand (Himmelwright et al., 1978). There is no direct evidence, however, that nitrite is a bridging ligand in GHM Hc. In fact, the unpaired electron is completely localized on the Cu(II) in the binuclear Cu(I)−Cu(II) center [Westmoreland et al. (1989) and references cited therein]. The similarity of EPR and ESEEM spectra of *C. maenas* Cu(II)-Hc-NO_2^- and GHM Hc suggests that even if Cu(I) in GHM Hc is bound to a bridging nitrite, this binding has little effect on the coordination geometry of the Cu(II). Alternatively, nitrite may not be bound to Cu(I) at all.

A hypothesis that could rationalize the observed high affinity for nitrite when the second metal ion is present in the active site could be the formation of a hydrogen bond between the non-coordinating oxygen of nitrite and a protein substituent only when Cu(I) is in the adjacent site. A direct analysis of the binding mode for nitrite in all these derivatives of Hc, however, is compromised by the lack of a spectroscopic feature associated with the coupling of nitrite to copper.

REFERENCES

Abragam, A., & Bleaney, B. (1970) in *Electron Paramagnetic Resonance of Transition Metal Ions*, pp 455−469, Clarendon Press, Oxford, UK.

Bannister, W. H., & Wood, E. J. (1971) *Comp. Biochem. Physiol. 40B*, 7−18.

Belford, R. L., & Nilges, M. J. (1979) *Proceedings of the International Paramagnetic Resonance Symposium, 21st*, Rocky Mountain Conference, Denver, CO.

Beltramini, M., Ricchelli, F., & Salvato, B. (1984) *Inorg. Chim. Acta 92*, 219−227.

Brown, J. M., Powers, L., Kincaid, B., Larrabee, J. A., & Spiro, T. G. (1980) *J. Am. Chem. Soc. 103*, 984−986.

Bubacco, L., Magliozzo, R. S., Beltramini, M., Salvato, B., & Peisach, J. (1992) *Biochemistry 31*, 9294−9303.

Cornelius, J. B., McCracken, J., Clarkson, R. B., Belford, R. L., & Peisach, J. (1990) *J. Phys. Chem. 94*, 6977−6982.

Eickman, N. C., Himmelwright, R. S., & Solomon, E. I. (1979) *J. Am. Chem. Soc. 76*, 2094−2098.

Ellerton, D. H., Ellerton, N. F., & Robinson, H. A. (1983) *Prog. Biophys. Mol. Biol. 41*, 143−248.

Flanagan, K. L., & Singel, D. J. (1987) *J. Chem. Phys. 87*, 5606−5616.

Freedman, T. B., Loehr, J. S., & Loehr, T. M. (1976) *J. Am. Chem. Soc. 98*, 2809−2815.

Godden, J. W., Turley, S., Teller, D. C., Adman, E. T., Liu, M. Y., Payne, W. J., & LeGall, J. (1991) *Science 253*, 438−442.

Goldfarb, D., Fauth, J. M., Tor, Y., & Shanzer, A. (1991) *J. Am. Chem. Soc. 113*, 1941−1948.

Hazes, B., Magnus, C., Bonaventura, C., Bonaventura, J., Dauter, Z., Kalk, K. H., & Hol, W. G. J. (1993) *Protein Sci. 2*, 567−619.

Henderson, T. A., Hurst, G. C., & Kreilick, R. W. J. (1985) *J. Am. Chem. Soc. 107*, 7299−7303.

Himmelwright, R. S., Eickman, N. C., & Solomon, E. I. (1978) *Biochem. Biophys. Res. Commun. 81*, 243−247.

Hochstein, L. I., & Tomlinson, G. A. (1988) *Annu. Rev. Microbiol. 42*, 231−261.

Howes, B. D., Abraham, Z. H. L., Lowe, D. J., Brüser, T., Eady, R. R., & Smith, B. E. (1994) *Biochemistry 33*, 3171−3177.

Hurst, G. C., Henderson, T. A., & Kreilick, R. W. J. (1985) *J. Am. Chem. Soc. 107*, 580−594.

Jiang, F., McCracken, J., & Peisach, J. (1990) *J. Am. Chem. Soc. 112*, 9035−9044.

Jiang, F., Conry, R. R., Bubacco, L., Tyeklar, Z., Jacobson, R., Karlin, K. D., & Peisach, J. (1993) *J. Am. Chem. Soc. 115*, 2093−2102.

Kosugi, N., Yokoyama, T., & Kuroda, H. (1984) *Chem. Phys. 104*, 449−453.

Lakowicz, J. R. (1986) *Principles of Fluorescence Spectroscopy*, p 44, Plenum Press, New York.

Lee, P. A., Citrin, P. H., Eisenberger, P. M., & Kincaid, B. M. (1981) *Rev. Mod. Phys. 53*, 769−806.

Libby, E., & Averill, B. A. (1992) *Biochem. Biophys. Res. Commun. 187*, 1529−1535.

Lin, C. P., Bowman, M. K., & Norris, J. R. (1986) *J. Chem. Phys. 85*, 56−62.

Linzen, B., Soeter, N. M., Riggs, A. F., Schneider, H. J., Shartau, W., Moore, M. D., Yocota, E., Behrens, P. Q, Nakashima, H., Takagi, T., Nemoto, T., Verijken, H. J., Bak, H. J., Beintema, A., Volbeda, A., Gaykema, W. P. J., & Hol, W. G. J. (1985) *Science 229*, 519−529.

Lytle, F., Sayers, D., & Stern, E. (1989) *Physica B 158*, 701−706.

Magliozzo, R. S., & Peisach, J. (1992) *Biochemistry 31*, 189−199.

Magliozzo, R. S., Bubacco, L., McCracken, J., Jiang, F., Beltramini, M., Salvato, B., & Peisach, J. (1995) *Biochemistry 34*, 1513−1523.

Maurice, A. M. (1981) Ph.D. Thesis, University of Illinois, Urbana, IL.

McCracken, J., & Friedenberg, S. (1994) *J. Phys. Chem. 98*, 467−473.

McCracken, J., Peisach, J., & Dooley, D. M. (1987) *J. Am. Chem. Soc. 109*, 4064−4072.

McCracken, J., Cornelius, J. B., & Peisach, J. (1989) in *Pulsed EPR: A new field of application* (Keijzers, C. P., Reijerse, E. J., & Schmidt, J., Eds.) pp 156−161, North Holland Publ., Amsterdam.

Mims, W. B. (1972) *Phys. Rev. B 5*, 2409−2419.

Mims, W. B. (1974) *Rev. Sci. Instrum. 45*, 1583−1591.

Mims, W. B. (1984) *J. Magn. Reson. 59*, 291−306.

Mims, W. B., & Peisach, J. (1978) *J. Chem. Phys. 69*, 4921−4930.

Mims, W. B., & Peisach, J. (1979) in *Biological Applications of Magnetic Resonance* (Shulman, R. G., Ed.) pp 221−269, Academic Press, New York.

Mims, W. B., & Peisach, J. (1981) in *Biological Magnetic Resonance* (Berliner, L. J., & Reuben, J., Eds.) Vol. 3, pp 213–263, Plenum, New York.
Mims, W. B., Peisach, J., & Davis, J. L. (1977) *J. Chem. Phys. 66*, 5536–5550.
Nilges, M. J. (1979) Ph.D. Thesis, University of Illinois, Urbana, IL.
Peisach, J., & Blumberg, W. E. (1974) *Arch. Biochem. Biophys. 165*, 691–708.
Peisach, J., Mims, W. B., & Davis, J. L. (1979) *J. Biol. Chem. 242*, 2847–2858.
Powers, L. (1982) *Biochim. Biophys. Acta 683*, 1–38.
Salvato, B., Ghiretti-Magaldi, A., & Ghiretti, F. (1974) *Biochemistry 13*, 4778–4783.
Salvato, B., Beltramini, M., Piazzesi, A., Alviggi, M., Ricchelli, F., Magliozzo, R. S., & Peisach, J. (1986) *Inorg. Chim. Acta 125*, 55–66.
Sano, M., Komorita, S., & Yamatera, H. (1992) *Inorg. Chem. 31*, 459–463.
Scheuring, E., Sagi, I., & Chance, M. R. (1994) *Biochemistry 33*, 6310–6315.
Schweiger, A. (1989) in *Advanced EPR, Applications in Biology and Biochemistry* (Hoff, A. J., Ed.) pp 243–276, Elsevier, Amsterdam.
Smith, T. A., Penner-Hahn, J. E., Berding, M. A., Doniach, S., & Hodgson, K. O. (1985) *J. Am. Chem. Soc. 107*, 5945–5955.
Tamburro, A. M., Salvato, B., & Zatta, P. (1977) *Comp. Biochem. Physiol. 55B*, 346–356.
Van der Deen, H., & Hoving, H. (1977) *Biochemistry 16*, 3519–3527.
Van Holde, K. E. (1967) *Biochemistry 6*, 93–99.
Westmoreland, T. D., Wilcox, D. E., Baldwin, M. J., Mims, W. B., & Solomon, E. I. (1989) *J. Am. Chem. Soc. 111*, 6106–6123.
Witters, R., Groeseneken, D., Jacobs, P., & Lontie, R. (1982) *J. Inorg. Biochem. 16*, 237–243.
Woolery, G. L., Powers, L., Winkler, M., Solomon, E. I., & Spiro, T. G. (1984) *J. Am. Chem. Soc. 106*, 86–92.

BI941403C